Journal of
Synchrotron
Radiation

ISSN 0909-0495

Received 8 April 2005
Accepted 21 June 2005

A new experimental cell for *in situ* and *operando* X-ray absorption measurements in heterogeneous catalysis

J.-S. Girardon,[a] A. Y. Khodakov,[a]* M. Capron,[a] S. Cristol,[a] C. Dujardin,[a] F. Dhainaut,[a] S. Nikitenko,[b] F. Meneau,[c] W. Bras[c] and E. Payen[a]

[a]Laboratoire de Catalyse de Lille, USTL, Bâtiment C3, 59655 Villeneuve d'Ascq, France, [b]Fonds Wetenschappelijk Onderzoek (FWO) DUBBLE CRG ESRF, BP 220, 38043 Grenoble CEDEX, France, and [c]Netherlands Organization for Scientific Research (NWO) DUBBLE CRG ESRF, BP 220, 38043 Grenoble CEDEX, France. E-mail: andrei.khodakov@univ-lille1.fr

A new X-ray absorption cell dedicated to *in situ* and *operando* experiments in heterogeneous catalysis has been built and tested. The cell consists of several boron nitride and stainless steel plates linked together using graphite seals. It allows the measurement of XANES and EXAFS spectra of heterogeneous catalysts within a wide range of photon energies in transmission mode under the flow of various oxidative and reductive gas mixtures at elevated temperatures. The cell is compact and easy to build. Catalysts are loaded into the cell as powders. The use of boron nitride and a small beam pathlength in the cell result in a low absorption of the X-ray beam at lower energies. The cell was tested by *in situ* characterizing cobalt species during oxidative and reductive pre-treatments of a silica-supported Fischer-Tropsch catalyst. An *operando* study of methanol conversion over alumina-supported molybdenum catalysts was also carried out.

Keywords: *in situ*; *operando*; XANES; EXAFS; supported catalysts; instrumentation; Fischer-Tropsch synthesis; methanol oxidation.

1. Introduction

Synchrotron-based X-ray absorption spectroscopy has been used over the last decades as a powerful method for local order characterization in dispersed and amorphous catalytic systems. In many cases the structural information can be collected *in situ* during different catalyst pre-treatments or catalytic reactions, when the catalyst is inaccessible to traditional surface analysis. The possibility of performing *in situ* measurements has led to the construction of several cells for XANES and EXAFS experiments (Dalla Betta *et al.*, 1984; Lytle *et al.*, 1985; Kampers *et al.*, 1989; Clausen & Topsoe, 1991; Pettiti *et al.*, 1999; Barton *et al.*, 1999; Odzak *et al.*, 2001; Braun *et al.*, 2003; Topsoe, 2003; Weckhuysen, 2003). The construction of those cells is often quite complex; several parts have to be specifically manufactured. Some X-ray cells require the catalyst to be pressed in the form of wafers or pellets. It is known, however, that making wafers and pellets from the original powder of the catalyst can significantly alter the catalyst structure. In addition, the gas flow dynamics in the cells using compressed wafers and pellets seem to be different from those obtained in a conventional laboratory catalytic reactor, where the catalyst is usually present as a dispersed powder.

The present work presents a new experimental cell designed in our laboratory for *in situ* and *operando* X-ray absorption studies. The cell is compact, inexpensive and can be easily manufactured and handled. Owing to the variable beam pathlength, the cell is well suited for measuring X-ray absorption spectra in a wide range of photon energies (7–20 keV). The experiments can be conducted at ambient and elevated temperatures under the flow of a large number of oxidizing or reducing gas mixtures. Similarly to real working catalysts, the sample is loaded into the cell as a powder. The performance of the new X-ray absorption cell was evaluated by studying the local order of cobalt atoms during oxidative and reductive treatment of silica-supported cobalt Fischer-Tropsch catalysts and the behaviour of alumina-supported molybdenum catalysts during methanol partial oxidation.

2. Design of the X-ray absorption cell

The new *in situ* X-ray absorption cell is displayed in Fig. 1. The cell consists of several plates of stainless steel and boron nitride linked together using graphite seals. The components of the cell are held together by eight screws. The use of homemade plates of boron nitride (made from bulk boron nitride; MCSE, Grade A) allows minimizing X-ray absorption

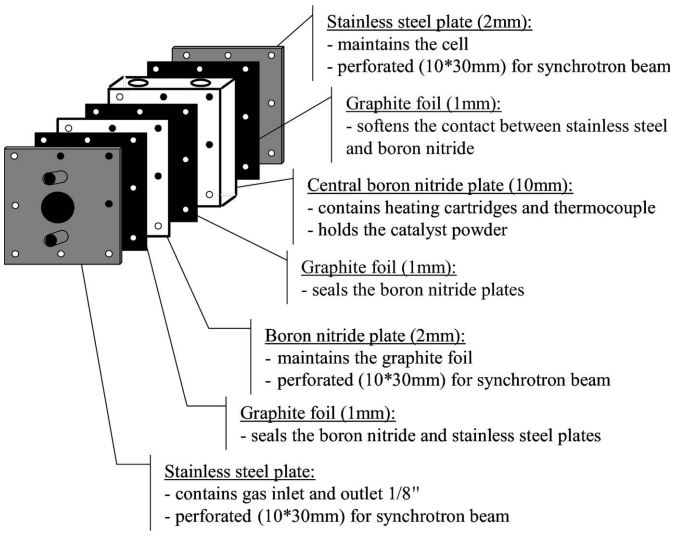

Figure 1
Experimental cell for *in situ* and *operando* X-ray absorption measurements.

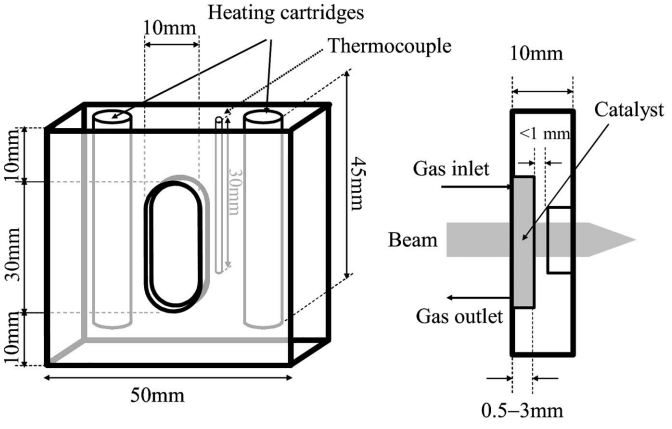

Figure 2
Central boron nitride plate – sample holder.

by the cell. To reduce further X-ray absorption by boron nitride at lower photon energies (~7 keV) the length of the beam path in boron nitride has to be reduced, and the plate was drilled from the rear side (Fig. 2). Thus, the thickness of boron nitride crossed by the beam was reduced to less than 1 mm. The cells with different pathlengths can be easily obtained by making a set of central boron nitride plates with different depths of the hollow. To perform X-ray absorption measurements, the boron nitride and stainless steel plates have to be assembled and sealed using graphite foils of thickness 2 mm (Carbone Lorraine). Our experiments have shown that the cell is leak-free at atmospheric pressure in pure oxygen or pure hydrogen at temperatures from ambient to 623 and 673 K, respectively. The catalyst for X-ray absorption measurements in the form of compacted powder is loaded into the hollow of the boron nitride plate (Fig. 2). The cell is equipped with a system of gas circulation, thermocouple and heating elements. The gas flow is introduced into the catalyst bed from the top of the cell; the gas outlet is located at the cell bottom. Two holes were drilled into each of the boron nitride plates and graphite foils (Fig. 1) to constitute the gas flow channel (one for the inlet and the other for the outlet). The catalyst container is oval-shaped. The gas flow from the top to the bottom through the catalyst powder is essential in the design of cells for *in situ* or *operando* X-ray absorption measurements. While the formation of preferential gas flow paths cannot be entirely ruled out in any experimental set-up, the vertical gas flow in the present cell, in contrast to the EXAFS cells with horizontal gas flow (Lytle *et al.*, 1985; Barton *et al.*, 1999), considerably reduces this possibility as well as the presence of empty spaces and inhomogeneity in catalyst powder. The preferential gas flow paths in the catalyst compromise the authenticity of the *in situ* and *operando* information, whereas the inhomogeneity of catalyst powder affects the quality of X-ray absorption spectra. The gas flow rates are controlled with electronic mass flow controllers (Brooks) assembled in a gas manifold. The cell is heated by two heating cartridges placed inside the boron nitride plate (sample holder, Fig. 2). Owing to the high thermal conductivity (30–100 $W\,m^{-1}\,K^{-1}$) of boron nitride, the heat is supplied uniformly to the catalyst. In order to ensure good thermal contact, the thermocouple is placed close to the catalyst sample in a hole drilled into the boron nitride plate. The *in situ* cell operates with a programmable temperature controller, which enables controlled temperature ramps to be performed in the range 293–673 K, with very low temperature gradients (<1 K). The internal volume of X-ray absorption was manufactured to 0.45 cm^3 with a depth of 0.15 cm (Fig. 2). The cell can be shielded and continuously purged with nitrogen if inflammable and explosive gases are used. Furthermore, in order to reduce or increase the residence time in *operando* experiments, the amount of catalyst loaded into the cell can be adjusted by making sample holders with different volumes of the hollow in the boron nitride plate. With all these settings, this X-ray absorption cell represents a real catalytic reactor. In order to test the quality of the cell for X-ray absorption experiments, we have recorded the spectrum of the $Al_2(MoO_4)_3$ reference compound in our new cell and the spectrum of $Al_2(MoO_4)_3$ crushed and compressed into a pellet as in a regular experiment. Fig. 3 shows that no artifacts are introduced to the absorption spectrum by the cell design.

3. Experimental

3.1. XAS measurements

The X-ray absorption spectra at the Co and Mo *K*-edge were measured at the European Synchrotron Radiation Facility (DUBBLE-CRG, Grenoble, France). Measurements were performed in transmission and two ionization chambers were used for X-ray detection. The Si(111) double-crystal monochromator was calibrated by setting the first inflection point of the *K*-edge spectrum of Co foil at 7709 eV or by setting the first inflexion point of the Mo foil *K*-edge spectrum at 19999 eV. The time of measuring an X-ray absorption spectrum (7600–8400 eV/19800–20800 eV) was about 40 min.

The X-ray absorption data were analyzed using the conventional procedure. The XANES spectra, after background correction, were normalized by the edge height. After subtracting metal atomic absorption, the extracted EXAFS signal was transformed without phase correction from **k** space to **r** space to obtain the radial distribution function.

3.2. Catalyst preparation

The supported cobalt–ruthenium Fischer-Tropsch catalyst was prepared using co-impregnation of Cabosil M5 silica (S_{BET} = 214 $m^2\ g^{-1}$) with aqueous solutions of cobalt acetate and ruthenium nitrosyl nitrate. The cobalt and ruthenium contents in the catalysts were 7.0 and 0.2 wt%, respectively. After impregnation, cobalt–ruthenium catalysts were dried overnight at 363 K. Then the catalyst was heated in a flow of air or hydrogen with a flow rate of 20 $cm^3\ min^{-1}$ and a temperature ramp of 60 K h^{-1}. The X-ray absorption spectra were measured in a gas flow at a desired temperature.

Mo/Al_2O_3 was prepared by incipient wetness impregnation of a high-specific-area ($\sim$500 $m^2\ g^{-1}$) alumina support with ammonium heptamolybdate solution [$Mo_7O_{24}(NH_4)_6.4H_2O$; Fluka, $\geq$99%], the amount of added heptamolybdate being adjusted for the preparation of a catalyst with 20 wt% Mo. After drying overnight at 373 K, the sample was calcined in air at 773 K for 3 h with a ramp rate of 40 K h^{-1}. Prior to the catalytic reaction, the catalyst was activated *in situ* at 623 K under an oxygen flow for 3 h.

4. X-ray absorption measurements

4.1. *In situ* XANES/EXAFS study of local cobalt coordination

The *in situ* XANES and EXAFS data measured at the cobalt *K*-edge during oxidative and reductive pre-treatments of cobalt–ruthenium catalyst using the new X-ray absorption cell are presented in Figs. 4(*a*) and 4(*b*). The X-ray absorption results were analysed using crystalline cobalt acetate hydrate, Co_3O_4, CoO, Co foil and α- and β-cobalt silicate as standard compounds. The XANES and EXAFS data of the standard compounds along with the information about their structures are available from our previous publications (Khodakov *et al.*, 1997, 1999; Girardon *et al.*, 2005). The XANES spectra and Fourier transform moduli of EXAFS were almost identical for impregnated cobalt–ruthenium catalyst and cobalt acetate (Fig. 4 and Girardon *et al.*, 2005). This suggests a similar octahedral Co–O local environment in the impregnated catalyst and in cobalt acetate. The pre-treatment in the flow of air at 373 K and 443 K leads to only minor changes in the XANES spectrum and Fourier transform modulus. This suggests that cobalt acetate remains the main cobalt phase after the pre-treatments at temperatures below 443 K.

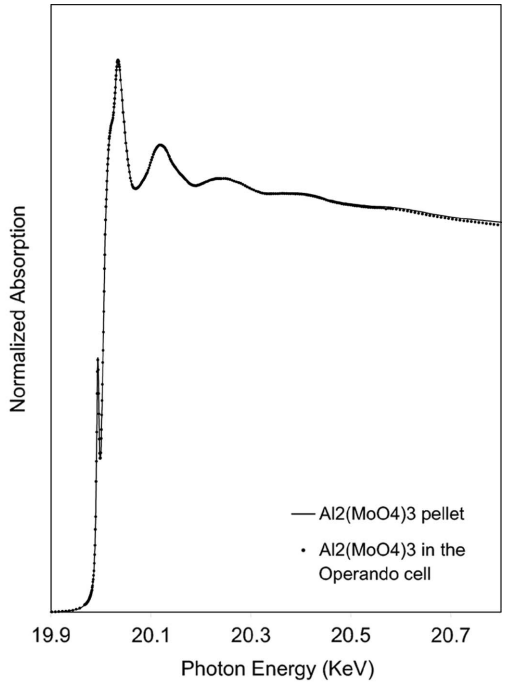

Figure 3
X-ray absorption spectra of $Al_2(MoO_4)_3$ reference compound measured in a regular experiment as a compressed pellet and in the new experimental cell.

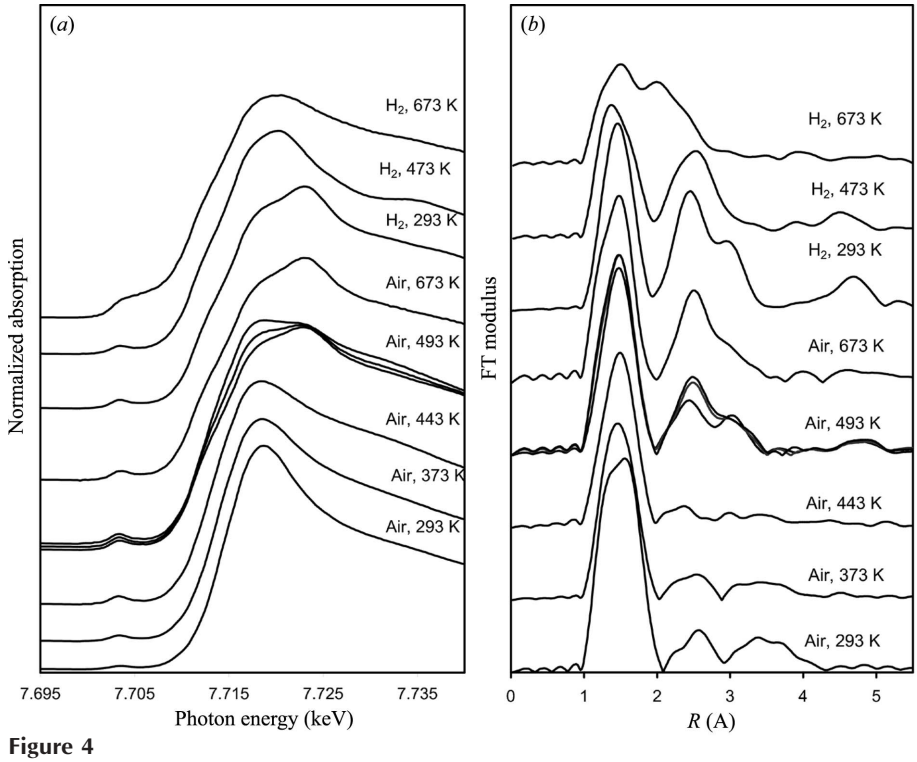

Figure 4
In situ XANES spectra (*a*) and moduli of Fourier transform of EXAFS (*b*) of cobalt catalysts measured during the pre-treatments in a flow of air or hydrogen.

Heating the cobalt–ruthenium catalyst in the air flow at 493 K results in a gradual evolution with time of the XANES spectrum and the modulus of the Fourier transform of the EXAFS (Figs. 4*a* and 4*b*). The observed transformation of the XANES spectrum and EXAFS is consistent with the decomposition of cobalt acetate. Our earlier study (Girardon *et al.*, 2005), carried out using calorimetric and thermogravimetric analysis, has shown that cobalt acetate decomposes in the flow of air at 493 K. The XANES spectrum and Fourier transform modulus of the EXAFS change only slightly with a temperature increase from 493 to 673 K. The analysis of X-ray absorption data for the catalyst pre-calcined at 493 and 673 K suggests that cobalt atoms situated in crystalline Co_3O_4 and amorphous α-cobalt silicate probably both contribute to the XANES and EXAFS signals. After oxidative pre-treatment the catalyst was cooled down to room temperature. After purging with nitrogen at 293 K, the catalyst was exposed to hydrogen flow. No significant modification of the XANES and EXAFS data were observed after treating the catalysts with hydrogen at room temperature. Figs. 4(*a*) and 4(*b*) show, however, that the pre-treatment of the catalyst in hydrogen at 473 K results in a modification of both the XANES spectrum and the EXAFS Fourier transform modulus. The X-ray absorption data can be fitted using CoO and α-cobalt silicate as reference compounds. This suggests that pre-treatment in hydrogen at 473 K results in a partial reduction of Co_3O_4 species to CoO. This observation is consistent with the previous data (van't Blik & Prins, 1986; Castner *et al.*, 1990; Ernst *et al.*, 1998) and our earlier results for cobalt-supported catalysts (Khodakov *et al.*, 1997, 2001). Heating the catalyst in hydrogen at 673 K results in further evolution of XANES and EXAFS data. The observed changes indicate the appearance of a Co metallic phase, which is probably due to the partial reduction in hydrogen of the CoO crystalline phase.

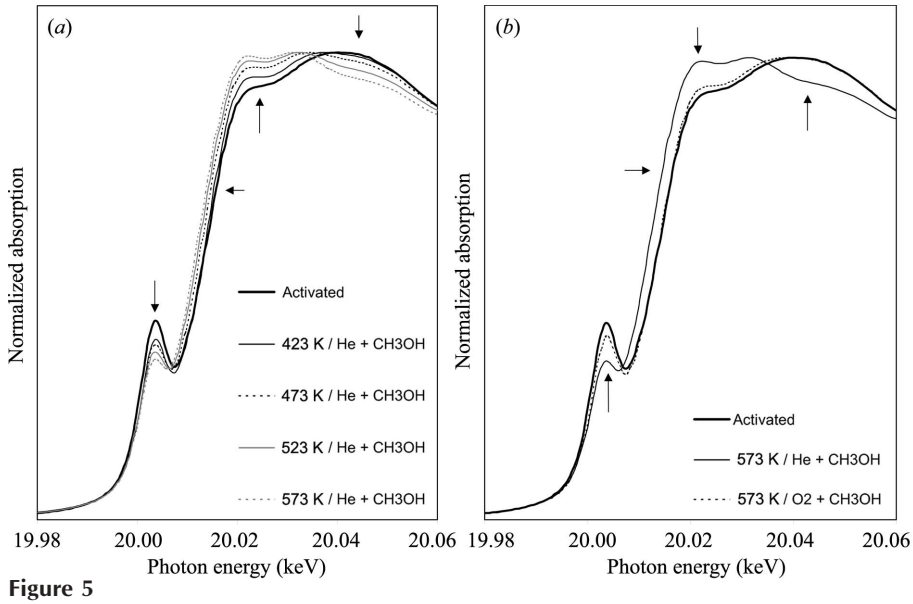

Figure 5
XANES spectra of Mo/Al_2O_3 at the Mo *K*-edge (*a*) under He + CH_3OH at different temperatures and (*b*) under different atmospheres at 573 K.

4.2. *Operando* study of methanol oxidation on Mo/Al_2O_3

Numerous studies have shown that methanol oxidation is very sensitive to the nature of active sites and can be used to study the acidic and oxidation properties of catalytic surfaces (Tatibouët, 1997; Briand *et al.*, 2000). The oxidative–reductive processes lead to oxidized species such as formaldehyde (F), formic acid (FA) and carbon oxides (CO_x) whereas acid–base functions mainly lead to the dehydration product (dimethylether, DME). Successive dehydrations of oxidation products can yield dimethoxymethane (DMM) or methylformate (MF). Hence, the distribution of the reaction products provides indications of the functionalities present on the catalyst surface. The catalyst was first activated in a pure oxygen flow at 623 K for 3 h. The spectrum of this activated catalyst, characteristic of Mo^{VI} in a tetrahedral environment according to Plazenet *et al.* (2002), is shown as a reference in Figs. 5(*a*) and 5(*b*). During the reaction, the methanol partial pressure was adjusted in the reaction mixture by a saturator cooled to 273 K. The effluent gas mixture was analysed by an online µ-gas chromatograph (SRA) equipped with Poraplot Q and 5A molecular sieve columns. Four-port valves allow bypassing of the saturator and/or switching between carrier gases so that XAS spectra and catalytic results can be recorded under different gas flow and/or different atmospheres. The Mo XANES spectra recorded at different temperatures under a He/CH_3OH mixture are presented in Fig. 5(*a*). A clear evolution of the XANES signal is seen (see arrows on the figure). This evolution can be attributed to the reduction of the active oxomolybdic phase by methanol. The temperature increase is indeed characterized by the production of a small amount of oxidation products as shown by gas-chromatography analysis. As there is no oxygen in the gas phase to reoxidize the reduced sites, the oxidative function of the catalyst quickly deactivates and no oxidation products can be detected under stationary conditions. The residual transformation of methanol to DME occurs on the acid sites of the alumina support. If helium is substituted by oxygen in the reactive mixture, the catalyst is regenerated as shown by the production of oxidation products (Fig. 6). It can be seen in Fig. 5(*b*) that this regeneration of the oxidative function is characterized by an almost complete restoration of the initial XAS signal obtained after activation of the catalyst. All these results are in agreement with previously obtained Raman and EPR data (Brandhorst *et al.*, 2005) and the signal obtained under the reductive atmosphere can be attributed to Mo^{V}. Detailed structural information is still to be extracted, but the intensity of the pre-edge peak seems to correlate with the quantity of Mo^{VI} in the sample. Indeed, a shift of the absorption edge towards low energies is observed along with a

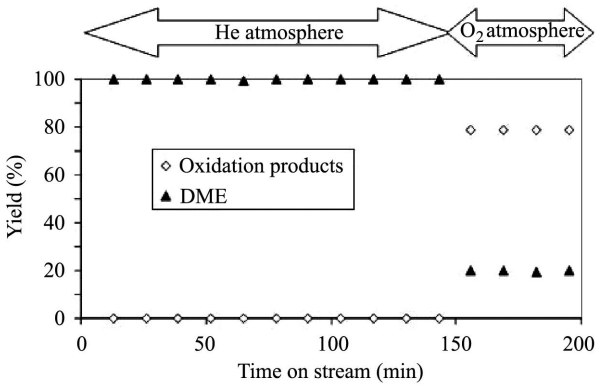

Figure 6
Yield of DME and oxidation products during methanol conversion at 573 K under helium and oxygen [$CH_3OH/He(O_2) = 0.04$, $W/F(CH_3OH) = 0.0674$ kg h mol^{-1}].

decrease of the pre-edge peak at each increase in the temperature. According to conventional interpretation, the absence of a pre-edge peak is characteristic of an octahedral environment around the absorber. The local environment around molybdenum centres should be closer to a perfect octahedron for the reduced species than for the oxidized ones. More subtle electronic effects (Joly *et al.*, 1999) cannot be ruled out however, and a more detailed analysis is required.

5. Conclusion

A new experimental cell for *in situ* and *operando* XANES and EXAFS experiments in heterogeneous catalysis has been designed. The two examples presented here show that this design is suitable for various environments, different temperatures and for many absorbers. Furthermore, no mechanical pre-treatment of the sample is required so that the catalyst can remain as a powder. Moreover, the experimental cell mimics realistically standard catalytic reactors.

The authors are indebted to M. Clément for valuable technical assistance in the cell design and construction. The authors acknowledge the European Synchrotron Radiation Facility (Grenoble, France) and the Netherlands Organization for Scientific Research (NWO) as well as Fonds Wetenschappelijk Onderzoek (FWO) for the use of the beamline for X-ray absorption measurements.

References

Barton, D. G., Soled, S. L., Meitzner, G. D., Fuentes, G. A. & Iglesia, E. (1999). *J. Catal.* **181**, 57–72.
Blik, H. F. J. van't & Prins, R. (1986). *J. Catal.* **97**, 210–218.
Brandhorst, M., Cristol, S., Capron, M., Dujardin, C., Vezin, H., Lebourdon, G. & Payen, E. (2005). *Catal. Today.* In the press.
Braun, A., Shrout, S., Fowlks, A. C., Osaisai, B. A., Seifert, S., Granlund, E. & Cairns, E. J. (2003). *J. Synchrotron Rad.* **10**, 320–325.
Briand, L. E., Farneth, W. E. & Wachs, I. E. (2000). *Catal. Today*, **62**, 219–229.
Castner, D. G., Watson, P. R. & Chan, I. Y. (1990). *J. Phys. Chem.* **94**, 819–828.
Clausen, B. S. & Topsoe, H. (1991). *Catal. Today*, **9**, 189–196.
Dalla Betta, R. A., Boudart, M., Foger, K., Löffler, D. G. & Sanchez-Arrieta, J. (1984). *Rev. Sci. Instrum.* **55**, 1910–1913.
Ernst, B., Bensaddik, A., Hilaire, L., Chaumette, P. & Kiennemann, A. (1998). *Catal. Today*, **39**, 329–341.
Girardon, J.-S., Lermontov, A. S., Gengembre, L., Chernavskii, P. A., Griboval-Constant, A. & Khodakov, A. Y. (2005). *J. Catal.* **230**, 348–361.
Joly, Y., Cabaret, D., Renevier, H. & Natoli, C. R. (1999). *Phys. Rev. Lett.* **82**, 2398–2401.
Kampers, F. W. H., Maas, T. M. J., van Grondelle, J., Brinkgreve, P. & Koningsberger, D. C. (1989). *Rev. Sci. Instrum.* **60**, 2636–2638.
Khodakov, A., Ducreux, O., Lynch, J., Rebours, B. & Chaumette, P. (1999). *Oil Gas Sci. Technol.* **54**, 525–536.
Khodakov, A., Griboval-Constant, A., Bechara, R. & Villain, F. (2001). *J. Phys. Chem. B*, **105**, 9805–9811.
Khodakov, A., Lynch, J., Bazin, D., Rebours, B., Zanier, N., Moisson, B. & Chaumette, P. (1997). *J. Catal.* **168**, 16–25.
Lytle, F. W., Greegor, R. B., Marques, E. C., Sandstrom, D. R., Via, G. H. & Sinfelt, J. H. (1985). *J. Catal.* **95**, 546–557.
Odzak, J. F., Argo, A. M., Lai, F. S., Gates, B. C., Pandya, K. & Feraria, L. (2001). *Rev. Sci. Instrum.* **72**, 3943–3945.
Pettiti, I., Gazzoli, D., Inversi, M., Valigi, M., Rossi, S. D., Ferraris, G., Porta, P. & Colonna, S. (1999). *J. Synchrotron Rad.* **6**, 1120–1124.
Plazenet, G., Payen, E., Lynch, J. & Rebours, B. (2002). *J. Phys. Chem. B*, **106**, 7013–7028.
Tatibouët, J.-M. (1997). *Appl. Catal. A*, **148**, 213–252.
Topsoe, H. (2003). *J. Catal.* **216**, 155–164.
Weckhuysen, B. M. (2003). *Phys. Chem. Chem. Phys.* **5**, 4351–4360.